



A Markov Chain Monte Carlo technique to sample transport and source parameters of Galactic Cosmic Rays

A. Putze¹, B. Coste², L. Derome², F. Donato³, and D. Maurin²

¹ The Oskar Klein Centre for Cosmoparticle Physics, Department of Physics, Stockholm University, AlbaNova, SE-10691 Stockholm, Sweden, e-mail: antje@fysik.su.se

² Laboratoire de Physique Subatomique et de Cosmologie, Université Joseph Fourier Grenoble 1, CNRS/IN2P3, Institut Polytechnique de Grenoble, 53 avenue des Martyrs, Grenoble, 38026, France

³ Department of Theoretical Physics and INFN, via Giuria 1, 10125 Torino, Italy

Abstract. We implemented a Markov Chain Monte Carlo (MCMC) technique within the USINE propagation package to estimate the probability-density functions for cosmic-ray transport and source parameters within an 1D diffusion model. From the measurement of the B/C and ³He/⁴He ratios as well as of radioactive cosmic-ray clocks, we calculate their probability density functions, with a special emphasis on the halo size L of the Galaxy and the local underdense bubble of size r_b . We also derive the mean, best-fit model parameters and 68% confidence intervals for the various parameters, as well as the envelopes of isotopic ratios. Additionally, we verify the compatibility of the primary fluxes with the transport parameters derived from the B/C analysis before deriving the source parameters. Finally, we investigate the impact of the input ingredients of the propagation model on the best-fitting values of the transport parameters (e.g., the fragmentation cross sections) in order to estimate the importance of the systematic uncertainties. We conclude that the size of the diffusive halo depends on the presence/absence of the local underdensity damping effect on radioactive nuclei. Moreover, we find that models based on fitting B/C are compatible with primary fluxes. The different spectral indices obtained for the propagated primary fluxes up to a few TeV/n can be naturally ascribed to transport effects only, implying universality of elemental source spectra. Finally, we emphasise that the systematic uncertainties found for the transport parameters are larger than the statistical ones, rendering a phenomenological interpretation of the current data difficult.

Key words. methods: statistical – cosmic rays

1. Introduction

The transport equation of Galactic cosmic rays (GCRs) is described in standard text-

book. It generally contains a source term (standard or exotic source/production), a diffusion term, and possibly convection, energy gain and losses, and catastrophic losses (fragmentation and decay). A full numerical treatment is generally required to solve the transport equation.

Send offprint requests to: A. Putze

However, analytical (or semi-analytical) solutions may be derived assuming a simplified description of the spatial dependence of the ingredients (e.g. the gas distribution) and some transport parameters. Such a semi-analytical solution has been implemented in the USINE propagation code¹ used below.

In the first paper Putze et al. (2009) of a series (Putze et al. 2009, 2010, 2011; Coste et al. 2011), we implemented a Markov Chain Monte Carlo (MCMC) to estimate the probability density function (PDF) of the transport and source parameters. This allowed us to constrain these parameters with a sound statistical method, to assess the goodness of fit of the models, and as a by-product, to provide 68% and 95% confidence level (CL) envelopes for any quantity we are interested in (e.g., B/C and $^3\text{He}/^4\text{He}$ ratios, primary cosmic-ray fluxes). The analysis was performed for a diffusion model, by considering constraints set by radioactive (on the halo size of the Galaxy) and primary nuclei (on the CR source parameters).

We summarise below the results we obtained in the diffusion model (normalisation K_0 and slope δ of the diffusion coefficient), with a halo size L , with minimal reacceleration (Alfvénic speed V_a), a constant Galactic wind perpendicular to the disc plane V_c (Jones et al. 2001), and a possible central underdensity of gas (of a few hundreds of pc) around the solar neighbourhood r_h (Donato et al. 2002).

2. Transport parameters

Secondary species in GCRs are produced during the CR journey from the acceleration sites to the solar neighbourhood, by means of nuclear interactions of heavier primary species with the interstellar medium. Hence, they are tracers of the CR transport in the Galaxy. Therefore, secondary-to-primary ratios, such as B/C and $^3\text{He}/^4\text{He}$, are suitable quantities to constrain the transport parameters for species $Z \leq 30$. For the parameter estimation of the above described transport equation (K_0 , δ , V_c and V_a), the usage in the past has been based

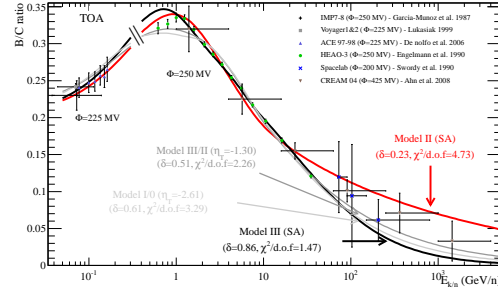


Fig. 1. Best-fit of the B/C ratio for different configurations: Model II ($V_c = 0$; red line), III (K_0 , δ , V_c , $V_a \neq 0$; black line), I/O ($V_c = V_a = 0$, $\eta_T \neq 1$; light grey line), and III/II ($V_c = 0$, $\eta_T \neq 1$; dark grey line). A more detailed description of this figure can be found in Maurin et al. (2010).

mostly on a manual or semi-automated (hence partial) coverage of the parameter space (e.g. Jones et al. 2001). More complete scans were performed, e.g., in Maurin et al. (2001), based on a grid analysis. The Markov Chain Monte Carlo is a step further to optimise the exploration of the parameter space.

Figure 1 illustrates the best-fit B/C ratio found from a χ^2 analysis, for different propagation models. In the following, we will focus on the full convection/reacceleration configuration of the diffusion model (Model III = $\{K_0, \delta, V_c, V_a\}$). This specific configuration leads to a rather large value of the diffusion slope δ (~ 0.86) since it includes convection ($V_c \sim 18.8$ km/s) (see Putze et al. 2010).

Figure 2 illustrates the power of the MCMC technique, which allows to retrieve the PDF of the parameters (here for a fixed halo size of $L = 4$ kpc). The symbols correspond to the best-fit values obtained from different parameterisations of the production cross-sections. Their spread illustrates the fact that systematic uncertainties in the calculation are already of the same order or larger than the statistical ones (i.e., the width of the PDFs). See Maurin et al. (2010) for more details. This will be an issue with the forthcoming high-precision measurements of AMS-02 on the ISS.

Most secondary-to-primary ratios have $A/Z \sim 2$, and in that respect, $^3\text{He}/^4\text{He}$ is unique since it probes a different regime and allows to address the issue of the ‘universality’ of prop-

¹ <http://lpsc.in2p3.fr/usine>

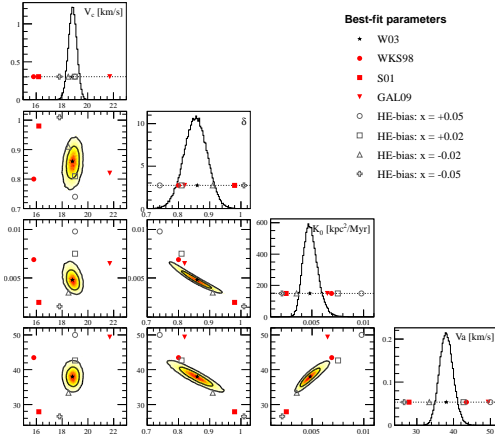


Fig. 2. PDF of the transport parameters as obtained in Putze et al. (2010), along with the best-fit values for different production cross-section sets: Webber et al. (2003, W03), black stars; Webber et al. (1998, WKS98), red dots; Soutoul (2001, S01), red squares; Galprop code v50.1p (2009, GAL09), red triangles; high-energy (HE) bias on W03, grey symbols. A more detailed description of this figure can be found in Maurin et al. (2010).

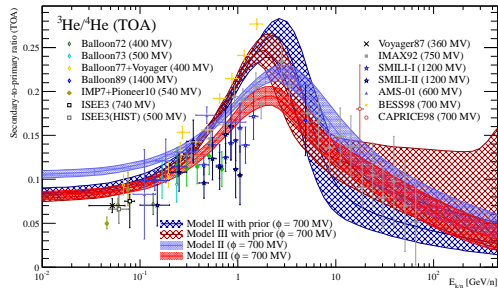


Fig. 3. Top-of-atmosphere (TOA, modulated at 700 MV) envelopes at 95% CL for the secondary-to-primary ${}^3\text{He}/{}^4\text{He}$ ratio for Model II and III with and without a prior on the source parameters.

agation histories. In our analysis of recent data (Coste et al. 2011), which is shown in Fig. 3 together with the envelopes at 95% CL, we find that the constraints obtained with ${}^3\text{He}/{}^4\text{He}$ on the transport parameters are competitive with those set by the B/C ratio. Moreover, the high abundance of the ${}^3\text{He}/{}^4\text{He}$ data make them a powerful alternative to the standard B/C analysis, so that the measurement of ${}^1\text{H}$, ${}^2\text{H}$, ${}^3\text{He}$, and ${}^4\text{He}$ should be a prime target for AMS-02.

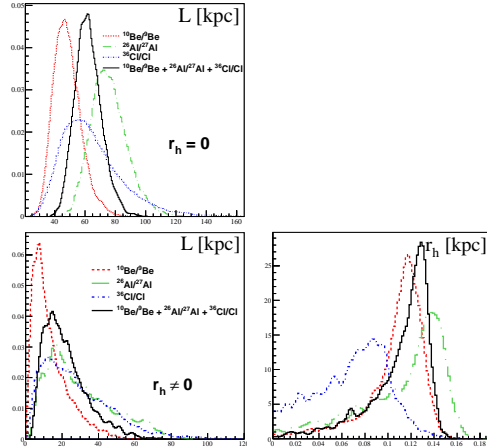


Fig. 4. Marginalised posterior PDFs of L for $r_h = 0$ (top panel) and L and r_h (bottom panels). The four curves result from the combined analysis of B/C plus separate or combined isotopic ratios of radioactive species.

3. Halo size L from radioactive nuclei

The typical distance travelled in a diffusive process in a finite time t is given by $l_{\text{rad}} \sim \sqrt{Kt}$, where K is the diffusion coefficient. For a β -decay unstable secondary species, it means that at low energy (using a typical value for the diffusion coefficient), these nuclei cannot travel farther than a few hundreds of parsecs: they do not feel the halo size L and are only sensitive to the diffusion coefficient K . In principle, this lifts the degeneracy between K_0 and L (seen from the analysis of the stable secondary-to-primary ratio). However, things are not as simple when we have a closer look at the hundred-of-parsec scale. It happens that there is no target to produce these species in the solar neighbourhood: we live in a local bubble. This lack of targets affects their flux (Donato et al. 2002). We find (see Putze et al. 2010) that the diffusion model including reacceleration and convection favours an underdense bubble of $r_h = 120^{+20}_{-20}$ pc (consistent with direct observations of the local cavity) and $L = 8^{+8}_{-7}$ kpc using ${}^{10}\text{Be}/{}^9\text{Be}$ data (see Fig. 4). The results from the combined analysis of B/C plus separate or combined isotopic ratios of radioactive species are shown in Fig. 4.

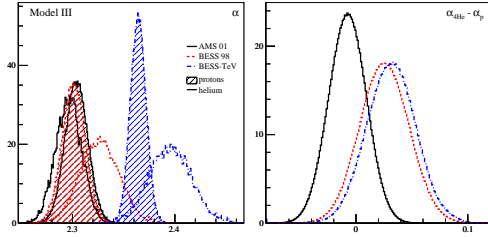


Fig. 5. Left panel: PDF of the source slope α for p (unfilled histograms) and He (hatched histograms). Right panel: PDF for $\alpha_{\text{He}} - \alpha_{\text{p}}$. The colour code corresponds to three experimental data used: AMS-01 (solid black line), BESS98 (dashed red lines), and BESS-TeV (dash-dotted blue lines).

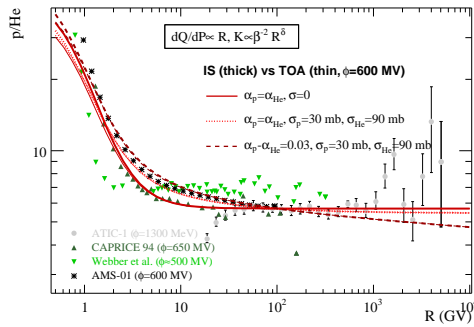


Fig. 6. p/He ratio as a function of rigidity. The lines show toy-model calculations with the destruction rate σ set to 0 (solid lines), set to its required value (dotted lines), plus a difference in the spectral index of p and He (dashed lines) for interstellar (IS, thick lines) and top-of-atmosphere (TOA, thin lines) fluxes.

4. Source parameters

The primary flux data alone are unable to select any particular propagation model, as the transport and source parameters are degenerate (Putze et al. 2011). We thus have to fit simultaneously the primary fluxes and secondary-to-primary ratios. Below, we adopt a different approach: we select only a few propagation models (fitting well the B/C ratio and shown in Fig. 1), and restrict the parameter space to the source parameter space only.

The most important parameter is the source slope α . Figure 5 shows the PDF of α for the best-measured primary species, i.e. p and He,

as well the difference of slope between these two species: $\alpha_{\text{p}} - \alpha_{\text{He}}$ is consistent with 0. Actually, the shape of the p/He ratios, when plotted as a function of the kinetic energy per nucleon, is driven by the solar modulation effect (not shown here). But the same ratio plotted as a function of the rigidity minimises the effect of the solar modulation, and is well adapted to probe the values of $\alpha_{\text{p}} - \alpha_{\text{He}}$. This is illustrated in Fig. 6, where a simple toy model was used to reproduce the experimental data. A difference of spectral index between p and He is also not supported by the ratio, in agreement with the direct fits to p and He fluxes.

We have also studied heavier primary nuclei spectra, whose relevant destruction rate on the ISM increases roughly with atomic number. The different spectral indices for the propagated primary fluxes up to a few TeV/n can be ascribed to transport effects only, implying universality of elemental source spectra. See Putze et al. (2011) for more details.

5. Conclusions and perspective

We have shown that the use of an MCMC technique is very powerful to study the source and transport parameters. The AMS-02 experiment should provide data with an unprecedented accuracy, and the MCMC technique will be a key tool to interpret them.

Acknowledgements. A. P. is grateful for financial support from the Swedish Research Council (VR) through the Oskar Klein Centre.

References

- AMS-collaboration (2010), *ApJ* **724**, 329
- Coste, B. et al. (2011), *arXiv:1108.4349*
- Donato, F. et al. (2002), *A&A* **381**, 539
- Jones, F. C. et al. (2001), *ApJ* **547**, 264
- Maurin, D. et al. (2001), *ApJ* **555**, 585
- Maurin, D. et al. (2010), *A&A* **516**, A67
- Putze, A. et al. (2009), *A&A* **497**, 991
- Putze, A. et al. (2010), *A&A* **516**, A66
- Putze, A. et al. (2011), *A&A* **526**, A101